Received: 26 August 2020 | Revised: 5 November 2020

DOI: 10.1002/biot.202000366

Biotechnology Journal

RESEARCH ARTICLE

Selective ene-reductase immobilization to magnetic nanoparticles through a novel affinity tag

Alexander A. Zanker | **Nadim Ahmad** | **Tuan Hoang Son** | **Sebastian P. Schwaminger** | **Sonja Berensmeier**

Bioseparation Engineering Group, Department of Mechanical Engineering, Technical University of Munich, Garching, Germany

Correspondence
Sonja Berensmeier, Technical University of Munich, Department of Mechanical Engineering, Bioseparation Engineering Group, Boltzmannstr, 15, 85748 Garching, BY, Germany.
Email: s.berensmeier@tum.de

Abstract

Background: Magnetic nanoparticles (MNPs) are becoming more important as carriers, because of their large specific surface area and easy separability. They are increasingly used in enzyme technology, diagnostics, and drug delivery.

Major results: For the directed and almost irreversible immobilization of proteins on MNPs, we have developed a new selective $(His\text{-}Arg)_4$ peptide-tag, that binds fusion proteins directly from an *E. coli* cell lysate to non-functionalized, low-cost MNPs. Using the immobilization of an ene-reductase as an example, we could demonstrate that the fusion with this tag increases thermostability without reducing overall activity (ER w/o tag: $t_{1/2}$ = 3.7 h, $(HR)_4$-ER: $t_{1/2}$ = 9.9 h). Immobilization by adsorption in Tris buffer resulted in very high enzyme loads with approx. 380 mg g^{-1} and 67% residual activity. The immobilization on the MNPs allowed a fast concentration, buffer exchange, and reuse. While about 50% of the activity was lost after the first reuse, we were able to show that the activity did not decrease further and was stable for another nine cycles.

Conclusion: According to our studies, our tag highly works for any kind of immobilization on MNPs and holds the potential for enzyme immobilizations as well as for drug delivery and sensors.

KEYWORDS
affinity tag, ene-reductase, enzyme immobilization, iron oxides, magnetic nanoparticles

1 | INTRODUCTION

Magnetic nanoparticles are used in all kinds of applications, such as enzyme immobilization, bioimaging, biosensors, drug delivery, enrichment of bacteria, and many more.[1–5] The high specific surface areas combined with the possibility of magnetic separation, are excellent prerequisites for immobilization purposes.[5–7] While porous supports have high specific surface areas as well, they can have mass transfer limitations, and thus, nanoparticles can outperform them.[5,8–10] Proteins can be immobilized on nanoparticles by physical adsorption or covalent linkage.[7,11] On the one hand, the covalent linkage is often accompanied by a high loss of protein activity and more complex immobilization protocols; on the other hand, weak physical adsorption can result in protein leaching.[5,11] However, adsorption through affinity tags proves to be an alternative to non-specific physical adsorption.[12] Their high affinity to the support material allows for combining immobilization and purification.[5,13] Whole proteins (like

Abbreviations: $(HR)_4$, dipeptide histidine-arginine repeated four times; AEX, anion exchange chromatography; Arg, arginine; BCA, bicinchoninic acid; ER, ene-reductase; ER w/o tag, ene-reductase without a tag; FMN, flavin mononucleotide; GFP, green fluorescent protein; His, histidine; HPLC, high-performance liquid chromatography; IMAC, immobilized metal affinity chromatography; Lys, lysine; MNPB, bound proteins on magnetic nanoparticles; MNPs, magnetic nanoparticles; MNPS, supernatant of magnetic nanoparticles after magnetic separation; MNPW, wash supernatant of magnetic nanoparticles after magnetic separation; NADH, nicotinamide adenine dinucleotide; NADPH, nicotinamide adenine dinucleotide phosphate; SDS-PAGE, sodium dodecyl sulfate-polyacrylamide gel electrophoresis; SEC, size exclusion chromatography; TBS, Tris-buffered saline

the HaloTag) or small peptide sequences (e.g., His-tag, Strep-Tag) can be used as affinity tags.[14–16] Using whole proteins as affinity tags often leads to a compromised activity of the fused partner, due to their size.[17] Thus, the usage of smaller affinity tags seems reasonable. Most affinity tags need specific counterparts for adsorption, for example, streptavidin-based tags bind to immobilized biotin.[15,18] Thus, an expensive surface modification is required for most affinity tags. Tags with high affinity to non-functionalized surfaces overcome this problem. The E_6-tag (Glu-tag), for instance, was successfully used as an affinity tag for non-functionalized MNPs and a successful purification of GFP-E_6 with MNPs was demonstrated.[19] Aside from the negatively charged E_6-tag, the positively charged peptides indicate a high affinity to MNPs as well.[20] Blank-Shim et al. observed high binding scores for the basic amino acids (Arg, Lys, His) in Tris, phosphate, and citrate buffers.[20] These findings led to the design of the here presented $(HR)_4$-tag, His-Arg-His-Arg-His-Arg-His-Arg, which has a more optimized selective and strong binding behavior.

The existence of histidines and arginines in one tag promises an advantageous, novel combination, which has the benefits of binding to divalent metal cations via the histidines and being polycationic, thus, increasing electrostatic interactions via the arginines. The $(HR)_4$-tag was fused to an enzyme to investigate the suitability as an enzyme immobilization tag. Therefore, the activity as well as the enzyme immobilization was investigated. We chose an ene-reductase (ER, EC 1.6.99.1) as a model enzyme for two main reasons. Firstly, ene-reductases are industrially relevant, because they are used for asymmetric synthesis.[21] Often used as whole-cell biocatalysts, these enzymes reduce activated C=C bonds *trans*-specifically; thus, generating chiral molecules.[22,23] The usage of ERs in the chemical industry is favorable since no use of metals is necessary and the reactions are performed under mild conditions with high stereoselectivities.[24,25] The second reason is due to its "complexity." It is an enzyme, which needs a cofactor (NADH), bears a prosthetic group (flavin mononucleotide [FMN]), and catalyzes reactions with a ping-pong bi-bi mechanism.[26] When our immobilization strategy works for such 'complex' enzymes, it is highly likely that it also works for less complex enzymes. We investigate the immobilization of an ene-reductase having the novel $(HR)_4$-tag to cheap non-functionalized MNPs. The immobilization of the ene-reductase on MNPs allows the reuse and simplified handling of oxidoreductases with this immobilization approach. The binding behavior of $(HR)_4$-ER on MNPs, the relative activities after immobilization, and the reusability of the immobilized enzyme are presented. Moreover, we compare the immobilization of $(HR)_4$-ER with the immobilization of the ER without this tag.

2 | MATERIALS AND METHODS

2.1 | Materials

The primers were synthesized by Eurofins (Eurofins Genomics GmbH, Germany) and the restriction enzymes were provided by NEB (New England Biolabs, USA) and used as supplied. The used Tris buffers were Tris (50 mM Tris-Base) and TBS (Tris-buffered saline, 50 mM Tris-Base, 137 mM NaCl, 2.7 mM KCl). The plasmids of the ene-reductase and GFP variants were obtained by Dr. Mähler and Dr. Blank- Shim, respectively. The ER used in our studies belongs to the Old yellow enzyme family (OYE, EC 1.6.99.1), which uses flavin mononucleotide (FMN) and NAD(P)H to reduce activated alkenes.[22] It originates from the cyanobacterium *Nostoc* sp. PCC7120 and was engineered by Mähler et al. to efficiently use NADH instead of NADPH as the cofactor.[27] The amino acid sequences of the $(HR)_4$-ER, ER w/o tag, GFP-$(RH)_4$, and GFP w/o tag are specified in the supplementary materials.

2.2 | Synthesis of magnetic nanoparticles

The MNPs were synthesized by co-precipitation of iron salts with sodium hydroxide following the protocol of Thomas et al.[28]

2.3 | Preparation of tagged and untagged proteins

The cultivation of the tagged proteins ($(HR)_4$-ER, ER w/o tag, GFP-$(RH)_4$, and GFP w/o tag), as well as the cloning of $(HR)_4$-ER and ER w/o tag, is detailed in the supporting information. $(HR)_4$-ER and GFP-$(RH)_4$ were purified with IMAC (immobilized metal affinity chromatography), whereas GFP w/o tag and ER w/o tag were purified using an AEX (anion exchange chromatography) and for ER w/o tag an additional purification step with a SEC (size exclusion chromatography). The detailed protocols are given in the supplementary materials.

2.4 | Protein analysis

The purified proteins were checked for purity via SDS-PAGE. For this, the samples were mixed with SDS loading buffer (containing 10 mM DTT) and denatured at 95°C for 5 min. The denatured samples were loaded onto a 15% or 12% polyacrylamide gel and an electrical field was applied. Additionally, the purity of ene-reductase or GFP compared to other proteins was validated by densitometry. The SDS-PAGE gel was scanned with the high-resolution scanner Amersham Typhoon NIR Plus (GE Healthcare Europe GmbH, Germany), and the densitometric analysis was done with its analysis software (Image Quant TL). The BCA assay was carried out with the Pierce BCA Protein assay kit (Thermo Fisher Scientific Inc., USA). The absorbance at 562 nm was measured after 30 min incubation at 37°C via an Infinite M200 Microplate Reader (Tecan Deutschland, Germany). Duplicates of each sample were measured. For HPLC analysis, 8 µL were injected and loaded onto a C4 column (Aeris, 3.6 µm, Widepore, 150 × 2.1 mm). The samples were analyzed twice with the following gradient (buffer A: double-distilled water with 20 mM TFA; buffer B: 100% acetonitrile with 20 mM TFA): The first step ran from 40% to 60% B in 10 column volumes, followed by three CV at 100% B and an equilibration step of five CV at 40% B. The sample concentrations were calculated employing an $(HR)_4$-ER standard present in the same buffer.

2.5 | Immobilization of tagged ER

Adsorption isotherms were carried out to investigate the maximum load of pure $(HR)_4$-ER to MNPs. The $(HR)_4$-ER was considered pure if the purity was above 95% according to densitometry. Different components (pure $(HR)_4$-ER, MNPs, buffer) were mixed yielding a final volume of 0.5 mL, 1 g L^{-1} MNPs and different $(HR)_4$-ER concentrations (0, 0.025, 0.05, 0.1, 0.25, 0.5, 0.75, 1.0, 1.5 and 2 g L^{-1}). These concentrations were obtained by mixing 0.25 mL $(HR)_4$-ER stocks (0, 0.05, 0.1, 0.5, 1, 1.5, 2, 3, 4 g L^{-1}) with 0.167 mL MNP (3 g L^{-1}) and 0.083 mL buffer. All components were present in the same buffer (50 mM Tris pH 7.0, pH 7.8 or TBS [50 mM Tris, 137 mM NaCl, 2.7 mM KCl] pH 7.0). The mixtures were incubated for 1 h at 16°C and 1200 rpm. The MNPs were separated from the supernatant by applying a magnetic field with a NdFeB hand-magnet. The supernatant was defined as *MNPS* (MNP supernatant). The MNPs were washed with the same buffer. A magnetic field was applied again, separating the MNPs from the supernatant. The supernatant was termed MNPW (MNP Wash). Finally, the MNPs were resuspended in the initial volume, defining the sample as MNPB (MNP bound). The MNPS and MNPW samples were analyzed by BCA assay and HPLC analysis. The load was calculated and subsequently fitted using the Langmuir model (see supporting information). All samples were prepared and analyzed as technical duplicates. The selectivity was qualitatively investigated by competitive adsorption isotherms and the experimental execution is detailed in the supplementary.

2.6 | Immobilization of untagged ER

The purified ene-reductase (0.3 or 0.5 g L^{-1}) was mixed with MNPs (1 g L^{-1}) and incubated (1 h, 16°C, 1000 rpm) in Tris buffer (50 mM, pH 7.0) in a total volume of 0.5 mL. Afterward, the MNPs were magnetically separated, the supernatant removed and the MNPs washed with Tris buffer (50 mM, pH 7.0). Finally, the MNPs were resuspended in Tris buffer (50 mM, pH 7.0) and could be used for further investigations. The load was calculated from the mass balance and was obtained by supernatant analysis via BCA assay.

2.7 | Determination of enzyme activity

The enzymatic activity of the ene-reductase was assessed by measuring the decrease of absorbance at 340 nm. This correlates with the decrease of NADH, which is oxidized to NAD^+. Hereby, the reaction rate was determined at 30°C. Unless otherwise stated, the activities were measured three times at 50 mM Tris pH 7.0, 10 mM maleimide, and 500 µM NADH. Reference samples (blanks) were the same samples with NADH and Tris but without maleimide. For adsorption isotherms, the activities were assessed in TBS (50 mM Tris, 137 mM NaCl, 2.7 mM KCl, pH 7.4) twice. The absorbance at 340 nm was determined every 40 s for 10 min. The enzyme activity was calculated in units (turnover of 1 µmol substrate per min). The turnover of NADH in µmol and finally the specific enzymatic activity ν_x (in U mg^{-1}) was calculated from the decreasing absorption ΔA_{340} by applying the Lambert-Beer law and considering the reaction volume V_R (in L) and applied enzyme mass m_E (in g).

$$\nu_x = \frac{\Delta A_{340} * V_R}{\Delta t * \varepsilon_{NADH} * d * m_E}$$

The absorptivity of NADH ε_{NADH} is 6220 L mol^{-1} cm^{-1} and the length of the light path is 0.59 cm. Only a linear decrease in absorption was used for the calculation of enzyme activity. For this case, linear means the linear decrease of absorption for at least 2 min showing an $R^2 > 0.99$. The enzyme kinetics for $(HR)_4$-ER was determined as published by Mähler.[27] The enzyme activity was determined at the corresponding Tris buffer (50 mM Tris pH 7.0, TBS pH 7.0, 50 mM Tris pH 7.8), maleimide (10 mM), and varied NADH concentrations (0 up to 1200 µM). For the kinetics, the assay was measured every 6 s for 10 min with a Multiscan FC Photometer (Thermo Fisher Scientific Inc., USA). The kinetic parameters (K_M and v_{max}) were estimated by nonlinear regression (Michaelis-Menten) using Matlab R2019b.

2.8 | Reusability

For reusability, the samples were repeatedly used, magnetically separated, and washed with Tris buffer (50 mM, pH 7.0). The MNP concentration was determined with a phenanthroline assay. The data were assessed as technical duplicates and measured three times (phenanthroline assay and enzyme assay: 50 mM Tris pH 7.0, 1 mM NADH, and 10 mM maleimide, 30°C). The enzymatic activities of cycles 1–4 were regressed as described above, the ones of cycles 5–9 were regressed over the whole 10 min. The carrier-specific (U g_{MNP}^{-1}) and particle-loss corrected enzyme activity was related to the enzymatic activity before reusing.

2.9 | Thermostability

The thermostability of $(HR)_4$-ER and ER w/o tag were assessed immobilized as well as free at three different temperatures (30, 40, and 50°C) and four time points (0, 2, 4, and 8 h). Each sample was analyzed as technical duplicates. The samples were incubated for 8 h at the corresponding temperatures. The enzyme activity (enzyme assay: 50 mM Tris pH 7.0, 500 µM NADH and 10 mM maleimide, 30°C), MNP concentration (phenanthroline assay), and protein concentration (BCA assay) were determined. The enzymet's activity was related to the corresponding specific enzymatic activity at 0 h. Immobilized samples were magnetically separated and washed at every point. The half-lives $t_{1/2}$ were calculated by $t_{1/2} = \frac{\ln(2)}{k}$. The coefficient k corresponds to the slope of linearly regressed data obtained from a (ln [relative activity] vs. time)-plot (see Figure S2).

2.10 | Analysis of MNPs

The concentration, zeta potential, and aggregation of the magnetic nanoparticles were determined. The precise experimental procedures are described in the supporting information.

3 | RESULTS AND DISCUSSION

3.1 | Magnetic nanoparticles as ideal carriers with a high specific surface area and saturation magnetization

The magnetic nanoparticles (MNPs) used for this study have been characterized in earlier work.[28] These MNPs were manufactured by co-precipitation, have a particle diameter of 10 nm, and a saturation magnetization of around 84 emu g^{-1} while showing no remanence.[28] A high specific surface area (101.5 m^2 g^{-1}) was obtained for MNPs synthesized with this approach.[29] These two features, the high specific surface area paired with the beneficial magnetic properties, imply that MNPs are ideal carriers for enzyme immobilization.

MNPs possess a positive zeta potential (11 mV) in Tris buffer (50 mM, pH 7.0), which correlates to results in Tris-buffered saline (TBS) at pH 7.4.[20] The aggregation behavior of the MNPs is similar in the used buffer system (Tris pH 7.8 [1251 nm], Tris pH 7.0 [1095 nm] and TBS pH 7.0 [1030 nm] [see Table S1]) and agrees with Schwaminger et al. who did not observe any hindrance for protein adsorption due to aggregation.[19]

3.2 | The $(HR)_4$-tag enables a purification with IMAC and enhances the overall stability

Enzyme kinetics of the $(HR)_4$-ER were analyzed to evaluate the influence of the tag on the enzyme activity. We could demonstrate that the activity of the ER having the tag was not compromised. The activity was similar under the three different buffer conditions (see Table S2). The $(HR)_4$-ER showed a high maximum activity ($k_{cat} = 28.1\ s^{-1}$, $v_{max} = 41.1$ U mg^{-1}) and a K_M ($K_M = 0.293$ mM) similar to the ER described in the literature ($k_{cat} = 29.1\ s^{-1}$ and a $K_m = 0.224$ mM).[27] This is not surprising, as the tag is very small (1.2 kDa) compared to other affinity tags such as the HaloTag (33 kDa).[30,31] There is a lower probability of small affinity tags to interfere with fused proteins than the larger affinity tags.[15]

Besides the advantageous property of being small, the $(HR)_4$-tag enables an easy purification with immobilized metal affinity chromatography (IMAC). Contrarily, two purification steps were necessary to purify the ER w/o tag: anion exchange chromatography (AEX) and size exclusion chromatography (SEC). Moreover, a stability-enhancing effect could be observed for the $(HR)_4$-tag when comparing the half-lives of $(HR)_4$-ER and ER w/o tag at 40°C. The $(HR)_4$-ER ($t_{1/2} = 9.9$ h) has an almost three times higher half-life than the ER w/o tag ($t_{1/2} = 3.7$ h) (see Table S3). This is also seen for long-term stability at 4°C (see Figure S3). Small polycationic tags such as the polylysine and polyarginine-tag can enhance the solubility, during expression, and of purified proteins.[32–34] We assume a similar behavior for our polycationic $(HR)_4$-tag. In conclusion, the $(HR)_4$-tag enhances the stability of the ene-reductase.

3.3 | Selective binding of an $(HR)_4$-tagged ene-reductase to MNPs with high loads

The ER was immobilized to MNPs with a simple protocol by just mixing pure ER and MNPs in Tris buffer. This protocol is illustrated in Figure 1 (see Figure 1).

The strong interactions of polyHis and polyArg-peptides with MNPs have already been described.[20,35] To proof the high affinity of our tag, we investigated the binding behavior of tagged proteins under competitive conditions. Only tagged proteins adsorb on the MNPs while the untagged do not adsorb (see Figure S4). Thus, the adsorption was triggered by the tag, and a switch of the tag to another protein (ER → GFP) evokes the same selective binding. This selectivity gives a big advantage for direct one-step immobilization from complex *E. coli* lysate. The selective interactions can be triggered by the histidines and arginines in the tag. Yet, it is not clear to which extent which amino acid is involved. The chemical structure of the $(HR)_4$-tag is depicted in Figure 1 (see Figure 1).

Achieving high loads of enzymes on a carrier is an important property for immobilization, too.[5] Adsorption isotherms of $(HR)_4$-ER and MNPs were investigated analyzing the supernatant with HPLC and BCA assay. The results of the BCA assay are shown in the supplementary (see Figure S5 and Table S4) and reveal the same trends as the HPLC results shown below (see Figure 2).

All adsorption isotherms show similar behavior, which can be described by the Langmuir model (see Figure 2). The steep increase of the load, which then levels off, is also documented.[36–38] The steep increase results in a low K_D value, which indicates a high affinity for all buffer conditions. These K_D-values are in the same range as other affinity-tagged GFP variants binding to iron oxide nanoparticles.[19,35]

Depending on the different buffer conditions, the order of the maximum loadings q_{max} are as follows: Tris pH 7.0 (0.383 g g^{-1}) > TBS pH 7.0 (0.243 g g^{-1}) > Tris pH 7.8 (0.114 g g^{-1}). The adsorption of $(HR)_4$-ER is strongly pH-dependent as expected and known from the literature.[37,39] However, the maximum adsorbed amount of enzyme is higher or in the same order of magnitude as references.[19,35,40–43] The rise of the load after the plateau can be caused by multilayer adsorption.[9,36,44] For comparison, an ene-reductase immobilized on EziG glass particles exhibited an up to 100 times smaller load of 0.004 g g^{-1}.[45]

3.4 | Activities of immobilized ene-reductase via the $(HR)_4$-tag is load dependent

In addition to high loads, the relative enzyme activity on the carrier is a decisive factor for enzyme immobilization. Investigation studies of

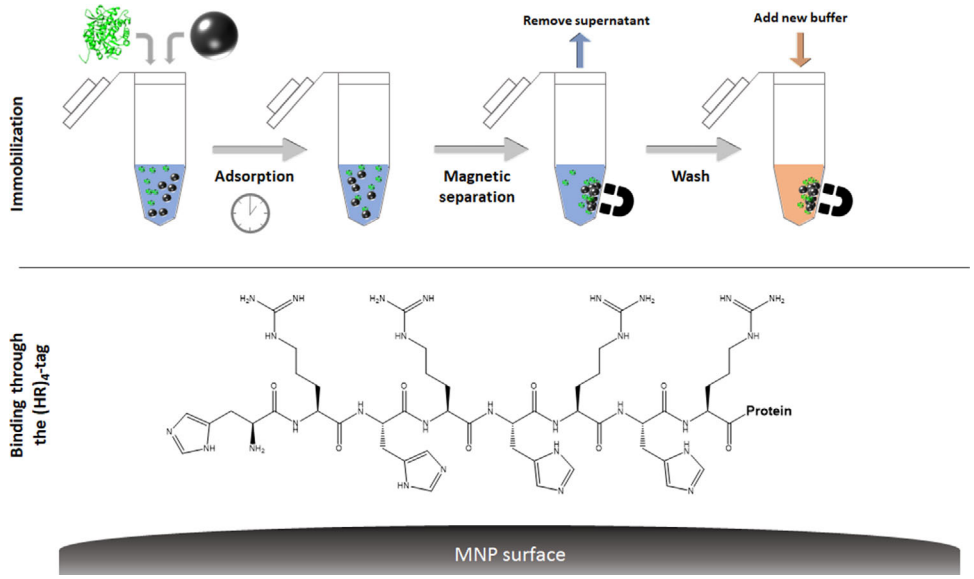

FIGURE 1 Schematic illustration of the enzyme immobilization (above) and the mechanism of binding through the N-terminal $(HR)_4$-tag fused to a protein (below). The immobilization protocol is easy and fast: Mixing of the ene-reductase (ER, green, homology model based on morphinone reductase, PDB: 2r14) with magnetic nanoparticles (MNP, grey balls) in an Eppendorf tube, incubating it for 1 h, magnetically separating the MNPs, discarding the supernatant and washing the remaining MNPs with a new buffer. Finally, the ER is immobilized to MNPs and ready for use. Below: Chemical structure of the N-terminal $(HR)_4$-tag adsorbing to the MNP surface

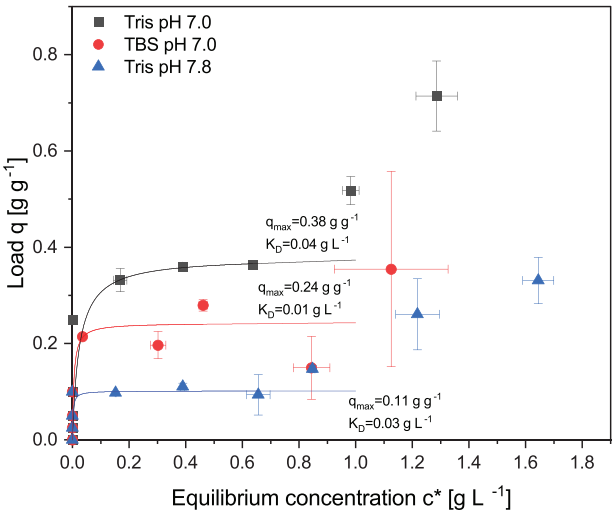

FIGURE 2 Adsorption isotherms of $(HR)_4$-ER with 1 g L^{-1} magnetic iron oxide nanoparticles (MNPs) at three different buffers (50 mM Tris pH 7.0, TBS pH 7.0, 50 mM Tris pH 7.8). Incubated for 1 h at 16°C 1200 rpm. Washing the MNPs after incubation and analyzing the supernatants with HPLC. Calculation of the load via mass balance. Standard deviation derived from technical duplicates measured twice with HPLC. The maximum load q_{max} and K_D were calculated assuming the Langmuir model for the equilibrium concentration range 0 to 0.8 g L^{-1}

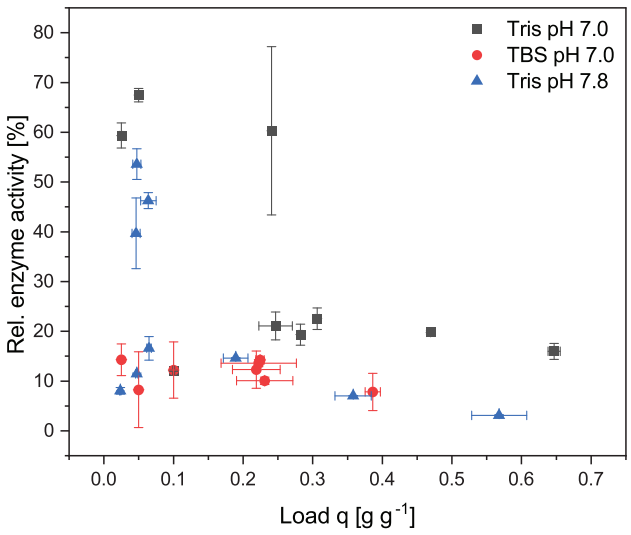

FIGURE 3 Relative enzyme activity of $(HR)_4$-ER bound to MNPs as a function of the load. The enzyme activity of the immobilized enzyme was related to the free enzyme's activity in the corresponding buffer. Applied ER concentration was mixed with 1 g L^{-1} MNPs. Enzymatic activities determined at TBS pH 7.4, 500 µM NADH, and 10 mM maleimide at 30°C. Measurements were performed as technical duplicates

MNPs with different assay components were performed to check for interferences. The studies clearly show no interference of the MNPs with NADH and maleimide (see Figure S6). The relative enzyme activities of $(HR)_4$-ER were determined at different loads (see Figure 3).

The highest relative activities were achieved for Tris pH 7.0 with the peak of activity being 67.5%. This activity optimum was ascertained at 0.05 g_{ER} g_{MNP}^{-1}, but the enzyme was still highly active at a higher load (0.25 g g^{-1}, 60%), too. For comparison, other enzymes physisorbed on MNPs show relative activities of 1% (dehalogenase), 40% (cellulase),

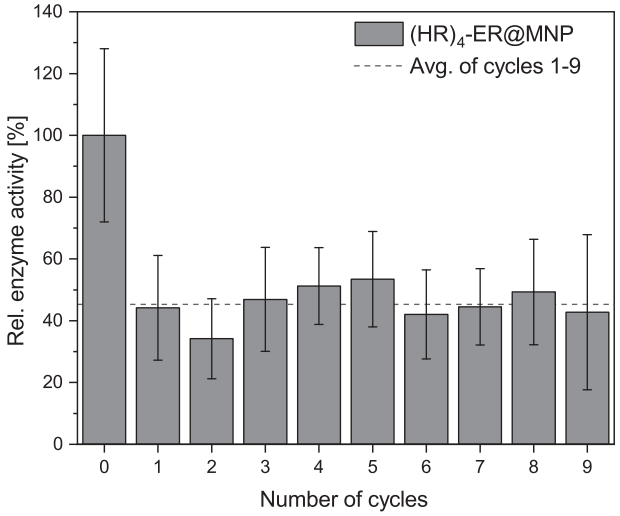

FIGURE 4 Reusability of $(HR)_4$-ER adsorbed to MNPs. Carrier-specific and particle-loss corrected enzyme activity related to the enzymatic activity before reusing. Repetition of the enzyme reaction, magnetically separating the MNP and washing. The MNP concentration was determined with phenanthroline assay. Performed as technical duplicates and measured twice (BCA assay) and three times (phenanthroline assay and enzyme assay: 50 mM Tris pH 7.0, 1 mM NADH, and 10 mM maleimide, 30°C)

and 71% (glycolate oxidase).[41–43] It seems that a loss of enzyme activity due to immobilization to MNPs, physisorbed, or covalently bound, must be tolerated.[40,42,43,46–48] At Tris pH 7.0, the relative activities of the ER show a decreasing trend with increasing loads, vice versa, low loads preserve a higher relative activity than larger loads. This kind of dependency is also described in the literature.[8,9,39] Even though low loads are favorable for high relative enzyme activities, industrial processes demand an optimum of high load and high relative activity. Thus, the use of 0.3 g L^{-1} $(HR)_4$-ER and 1 g L^{-1} MNPs is recommended for immobilization to obtain high loads and moderate relative activities.

Additionally, the $(HR)_4$-ER was compared with the relative activities of ER w/o tag on MNPs. Both immobilized ER variants exhibited similar enzyme activities (see Figure S7). Other groups published the immobilization of the ER with other approaches yielding recovered activities of around 50%.[45,49] It can be concluded that we have established a simple and fast immobilization protocol that allows high relative activities (up to 67.5%).

3.5 | Easy reusability of the $(HR)_4$-tagged ene-reductase immobilized to MNPs via magnetic separation

Besides easy processing, the main reason for enzyme immobilization is the reuse of the enzyme as shown for immobilized $(HR)_4$-ER in Figure 4.

$(HR)_4$-ER@MNP is reusable and remains very stable over several cycles with about 45.4% of the initial activity (average of cycles one to nine [see dashed line in Figure 4]). Only a large loss of activity was observed after the first cycle. This effect is known in literature and is attributed to biological reasons and inactivation of half of the enzymes after one cycle.[45,50,51] This assumption is supported by an experiment, where $(HR)_4$-ER adsorbed to MNPs was washed ten times and did not lose enzyme activity (see Figure S8). Here, the high particle loss on a small scale is significant (see Figure S9), but it should not be relevant on a technical scale, since higher quantities and high gradient magnetic separators with larger magnetic fields are used.[19,35] Ene-reductase immobilized in other approaches showed high reusability (>60%) after 10 cycles.[45,49] In conclusion, it was proven that $(HR)_4$-ER@MNPs was reusable by simply applying a magnetic field.

3.6 | Increased thermostability of the free and immobilized ene-reductase with the $(HR)_4$-tag

As thermostability is often enhanced by immobilization,[5,11] we compared the thermostability of immobilized $(HR)_4$-ER and ER w/o tag to their corresponding free variant at 30°C (see Figure S10), 40°C and 50°C (see Figure 5).

An increase in thermal stability was not yet observed at 30°C (see Figure S10) but could be observed at 40°C and 50°C. The immobilized $(HR)_4$-ER (73.6%) displayed higher activity than the free $(HR)_4$-ER (53.1%) at 40°C indicating an improvement of stability (see Figure 5). Furthermore, immobilized ER w/o tag (10.9% after 8 h) exhibited less activity than the corresponding free ER w/o tag (20.9% after 8 h) and in contrast to the $(HR)_4$-ER significantly less activity. At 50°C, the free variants lost their activity almost completely after 2 h, whereas the immobilized variants were still active. The immobilized variants even showed activity after 8 h (see Figure 5). This proves the enhanced thermostability due to immobilization on MNPs. Additionally, a stability-enhancing effect by the $(HR)_4$-tag is assumed and improved the thermostability of ER significantly.

4 | CONCLUSION

We were able to efficiently immobilize an ene-reductase with a novel affinity tag ($(HR)_4$-tag) to non-functionalized magnetic nanoparticles. The excellent properties of these MNPs indicate an optimal carrier for enzyme immobilization, meaning a cheap and simple synthesis without further modifications, a high specific surface area, and high saturation magnetization. In the course of our study, we got to know the extraordinary advantages of MNPs as a carrier system and want to highlight the simple and fast possibility of changing the buffer and concentrating the immobilized ER in particular. The $(HR)_4$-tag adsorbs to MNPs selectively, which was demonstrated by competitive adsorption isotherms. Even in a highly competitive environment, adsorption to MNPs is possible. High loads of $(HR)_4$-ER on MNPs were achieved by simply mixing the nanoparticles with purified enzymes. The highest load was observed for Tris pH 7.0 and we recommend it for other proteins with the $(HR)_4$-tag, similar pIs, and similar activity optima

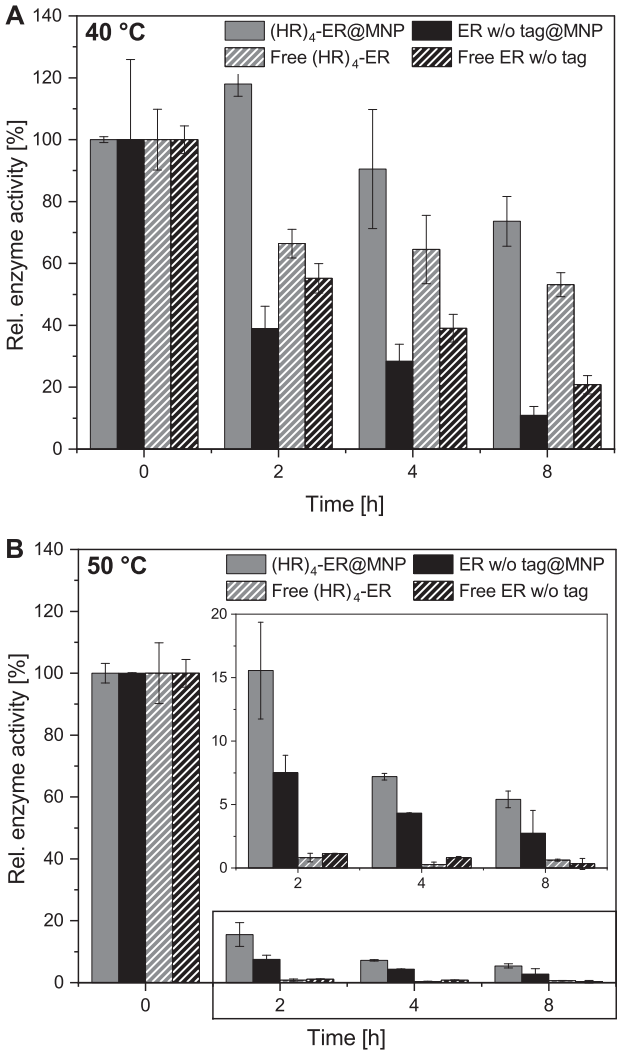

FIGURE 5 (A and B) The thermostability of $(HR)_4$-ER and ER w/o tag on MNPs and not bound (free) at two different temperatures (40 [Figure 5A] and 50°C [Figure 5B]). Performed as technical duplicates and measured three times (enzyme assay: 50 mM Tris pH 7.0, 500 µM NADH, and 10 mM maleimide, 30°C). Enzyme activity related to the corresponding specific enzymatic activity at 0 h. Immobilized samples were magnetically separated and washed at every time point

as optimal adsorption condition. Our easy immobilization protocol yielded high activities of immobilized $(HR)_4$-ER compared to the free enzyme. The adsorbed $(HR)_4$-ER was reusable several times. The high loss of particles between the reusability cycles can be overcome by using higher particle concentrations, which would lead to larger agglomerates, with easier separability using high gradient magnetic separators. The $(HR)_4$-tagged ER displayed a superior thermostability. In contrast to ER without tag, the $(HR)_4$-tag enabled an easy purification via IMAC, selective binding to MNPs, enhanced thermostability, and enhanced overall stability assuming a better solubility. According to our studies, this tag is highly suited for any kind of immobilization on MNPs. Beyond that, the selectivity of the $(HR)_4$-tag promises a purification with cheap magnetic nanoparticles. It seems that the $(HR)_4$-tag is an advantageous combination of a polyHis-tag (purification with IMAC, adsorption to divalent metal cations) and polyArg-tag (enhanced stability, polycationic), combining the best of both in one tag and enabling a strong interaction with MNPs. It is believed that the polycationic property of the $(HR)_4$-tag combined with the presence of histidines can enable strong binding to other surfaces as well, highly increasing the tag's versatility and application compared to other small tags. Moreover, it would be interesting how the tag works for proteins with high pI and other buffer systems.

ACKNOWLEDGMENTS

The authors would like to thank Prof. Kathrin Castiglione for the provided engineered ene-reductase and Dr. Christoph Mähler for the shared know-how regarding enzyme measurements and ene-reductase. We thank Dr. Silvia Blank-Shim and Yasmin Kaveh-Baghbaderani for the cloned GFP variants. We are thanking students Marina Telleria and Eduardo Palma for the purification of the tagged GFP variants. We are also grateful for the laboratory work of Swimmeryang Yu regarding the reusability experiment and the language editing by Tobias Steegmüller. Moreover, we are especially grateful for the financial support of the Federal Ministry of Education and Research (Grant number 031B0521A), which made this research possible.

Open access funding enabled and organized by Projekt DEAL.

CONFLICT OF INTEREST

Alexander A. Zanker, Sebastian P. Schwaminger, and Sonja Berensmeier filed a patent application.

DATA AVAILABILITY STATEMENT

The data that support the findings of this study are available from the corresponding author upon reasonable request.

AUTHOR CONTRIBUTIONS

Alexander Zanker: Conceptualization-Equal, Data curation-Lead, Formal analysis-Lead, Investigation-Equal, Project administration-Equal, Validation-Lead, Visualization-Lead, Writing-original draft-Lead, Writing-review & editing-Lead

Nadim Ahmad: Formal analysis-Supporting, Investigation-Equal, Visualization-Supporting

Tuan Hoang Son: Formal analysis-Supporting, Investigation-Equal, Visualization-Supporting

Sebastian Schwaminger: Conceptualization-Supporting, Formal analysis-Supporting, Project administration-Supporting, Supervision-Supporting, Validation-Supporting, Visualization-Supporting, Writing-original draft-Supporting, Writing-review & editing-Supporting

Sonja Berensmeier: Conceptualization-Equal, Funding acquisition-Lead, Project administration-Equal, Resources-Lead, Supervision-Lead, Writing-original draft-Supporting, Writing-review & editing-Supporting

ORCID

Alexander A. Zanker https://orcid.org/0000-0002-7855-2978
Sebastian P. Schwaminger https://orcid.org/0000-0002-8627-0807
Sonja Berensmeier https://orcid.org/0000-0002-4943-848X

REFERENCES

1. Wang, Z., Yue, T., Yuan, Y., Cai, R., Niu, C., & Guo, C. (2013). Preparation of immunomagnetic nanoparticles for the separation and enrichment of Alicyclobacillus spp. in apple juice. *Food Res Int.*, *54*(1), 302-310.
2. Dilnawaz, F., Singh, A., Mohanty, C., & Sahoo, S. K. (2010). Dual drug loaded superparamagnetic iron oxide nanoparticles for targeted cancer therapy. *Biomaterials*, *31*(13), 3694-3706.
3. Fredj, H. B., Helali, S., Esseghaier, C., Vonna, L., Vidal, L., & Abdelghani, A. (2008). Labeled magnetic nanoparticles assembly on polypyrrole film for biosensor applications. *Talanta*, *75*(3), 740-747.
4. Richards, D. A., Maruani, A., & Chudasama, V. (2017). Antibody fragments as nanoparticle targeting ligands: A step in the right direction. *Chem. Sci.*, *8*(1), 63-77.
5. Garcia-Galan, C., Berenguer-Murcia, Á., Fernandez-Lafuente, R., & Rodrigues, R. C. (2011). Potential of different enzyme immobilization strategies to improve enzyme performance. *Adv. Synth. Catal.*, *353*(16), 2885-2904.
6. Hyeon, J. E., Shin, S. K., & Han, S. O. (2016). Design of nanoscale enzyme complexes based on various scaffolding materials for biomass conversion and immobilization. *Biotechnol. J.*, *11*(11), 1386-1396.
7. Xu, J., Sun, J., Wang, Y., Sheng, J., Wang, F., & Sun, M. (2014). Application of iron magnetic nanoparticles in protein immobilization. *Molecules*, *19*(8),11465-11486.
8. Cao, L. (2006). Adsorption-based immobilization. In *Carrier-bound Immobilized Enzymes*. p. 53-168.
9. Magario, I., Ma, X., Neumann, A., Syldatk, C., & Hausmann, R. (2008). Non-porous magnetic micro-particles: Comparison to porous enzyme carriers for a diffusion rate-controlled enzymatic conversion. *J. Biotechnol.*, *134*(1–2), 72-78.
10. Jia, F., Narasimhan, B., & Mallapragada, S. (2014). Materials-based strategies for multi-enzyme immobilization and co-localization: A review. *Biotechnol. Bioeng.*, *111*(2), 209-222.
11. Hanefeld, U., Gardossi, L., & Magner, E. (2009). Understanding enzyme immobilisation. *Chem. Soc. Rev.*, *38*(2), 453-468.
12. Andreescu, S., Bucur, B., & Marty, J. - L. (2006). Affinity immobilization of tagged enzymes. In J.M. Guisan (Ed.), *Immobilization of Enzymes and Cells* (pp. 97-106), Totowa, NJ, Humana Press.
13. Nilsson, J., Larsson, M., Stahl, S., Nygren, P. A., & Uhlen, M. (1996). Multiple affinity domains for the detection, purification and immobilization of recombinant proteins. *J. Mol. Recognit.*, *9*(5–6), 585-594.
14. Young, C. L., Britton, Z. T., & Robinson, A. S. (2012). Recombinant protein expression and purification: A comprehensive review of affinity tags and microbial applications. *Biotechnol. J.*, *7*(5), 620-634.
15. Kimple, M. E., Brill, A. L., & Pasker, R. L. (2013). Overview of affinity tags for protein purification. *Curr. Protoc. Protein Sci.*, *73*, 9.9.1-9.9.23.
16. Terpe, K. (2003). Overview of tag protein fusions: From molecular and biochemical fundamentals to commercial systems. *Appl. Microbiol. Biotechnol.*, *60*(5), 523-533.
17. Zhao, X., Li, G., & Liang, S. (2013). Several affinity tags commonly used in chromatographic purification. *J. Anal. Methods Chem.*, *2013*, 581093-581093.
18. Schmidt, T. G. M., & Skerra, A. (2007). The Strep-tag system for one-step purification and high-affinity detection or capturing of proteins. *Nat. Protoc.*, *2*(6), 1528-1535.
19. Schwaminger, S. P., Blank-Shim, S. A., Scheifele, I., Pipich, V., Fraga-García, P., & Berensmeier, S. (2019). Design of interactions between nanomaterials and proteins: A highly affine peptide tag to bare iron oxide nanoparticles for magnetic protein separation. *Biotechnol. J.*, *14*(3), 1800055.
20. Blank-Shim, S. A., Schwaminger, S. P., Borkowska-Panek, M., Anand, P., Yamin, P., Fraga-García, P., … Berensmeier, S. (2017). Binding patterns of homo-peptides on bare magnetic nanoparticles: Insights into environmental dependence. *Sci. Rep.*, *7*(1), 14047.
21. Woodley, J. M. (2008). New opportunities for biocatalysis: making pharmaceutical processes greener. *Trends Biotechnol.*, *26*(6), 321-327.
22. Toogood, H. S., & Scrutton, N. S. (2018). Discovery, characterization, engineering, and applications of ene-reductases for industrial biocatalysis. *ACS Catal.*, *8*(4), 3532-3549.
23. Mähler, C., Burger, C., Kratzl, F., Weuster-Botz, D., & Castiglione, K. (2019). Asymmetric whole-cell bio-reductions of (R)-carvone using optimized ene reductases. *Molecules*, *24*(14), 2550.
24. Stuermer, R., Hauer, B., Hall, M., & Faber, K. (2007). Asymmetric bioreduction of activated C=C bonds using enoate reductases from the old yellow enzyme family. *Curr. Opin. Chem. Biol.*, *11*(2), 203-213.
25. Toogood, H. S., & Scrutton, N. S. (2014). New developments in 'ene'-reductase catalysed biological hydrogenations. *Curr. Opin. Chem. Biol.*, *19*, 107-115.
26. Breithaupt, C., Strassner, J., Breitinger, U., Huber, R., Macheroux, P., Schaller, A., & Clausen, T. (2001). X-ray structure of 12-oxophytodienoate reductase 1 provides structural insight into substrate binding and specificity within the family of OYE. *Structure (London, England : 1993)*, *9*(5), 419-429.
27. Mähler, C., Kratzl, F., Vogel, M., Vinnenberg, S., Weuster-Botz, D., & Castiglione, K. (2019). Loop swapping as a potent approach to increase ene reductase activity with nicotinamide adenine dinucleotide (NADH). *Adv. Synth. Catal.*, *361*(11), 2505-2513.
28. Thomas, J. A., Schnell, F., Kaveh-Baghbaderani, Y., Berensmeier, S., & Schwaminger, S. P. (2020). Immunomagnetic separation of microorganisms with iron oxide nanoparticles. *Chemosensors*, *8*(1), 17.
29. Schwaminger, S. P., García, P. F., Merck, G. K., Bodensteiner, F. A., Heissler, S., Günther, S., & Berensmeier, S. (2015). Nature of interactions of amino acids with bare magnetite nanoparticles. *J. Phys. Chem. C*, *119*(40), 23032-23041.
30. di Guan, C., Li, P., Riggs, P. D., & Inouye, H. (1988). Vectors that facilitate the expression and purification of foreign peptides in Escherichia coli by fusion to maltose-binding protein. *Gene*, *67*(1), 21-30.
31. Los, G. V., Encell, L. P., McDougall, M. G., Hartzell, D. D., Karassina, N., Zimprich, C., … Wood, K. V. (2008). HaloTag: A novel protein labeling technology for cell imaging and protein analysis. *ACS Chem. Biol.*, *3*(6), 373-382.
32. Paraskevopoulou, V., & Falcone, F. H. (2018). Polyionic tags as enhancers of protein solubility in recombinant protein expression. *Microorganisms*, *6*(2), 47.
33. Kato, A., Maki, K., Ebina, T., Kuwajima, K., Soda, K., & Kuroda, Y. (2007). Mutational analysis of protein solubility enhancement using short peptide tags. *Biopolymers*, *85*(1), 12-18.
34. Nautiyal, K., & Kuroda, Y. (2018). A SEP tag enhances the expression, solubility and yield of recombinant TEV protease without altering its activity. *N Biotechnol.*, *42*, 77-84.
35. Schwaminger, S. P., Fraga-García, P., Blank-Shim, S. A., Straub, T., Haslbeck, M., Muraca, F., … Berensmeier, S. (2019). Magnetic one-step purification of His-Tagged protein by bare iron oxide nanoparticles. *ACS Omega*, *4*(2), 3790-3799.
36. Carta, G., & Jungbauer, A. (2010). Adsorption equilibria. In *Protein Chromatography*. John Wiley & Sons. p. 145-160.
37. Shamim, N., Hong, L., Hidajat, K., & Uddin, M. S. (2006). Thermosensitive-polymer-coated magnetic nanoparticles: Adsorption and desorption of bovine serum albumin. *J. Colloid Interface Sci.*, *304*(1), 1-8.
38. Mahmoud, K. A., Male, K. B., Hrapovic, S., & Luong, J. H. T., Cellulose nanocrystal/gold nanoparticle composite as a matrix for enzyme immobilization. *ACS Appl. Mater. Interfaces*, 2009.*1*(7), 1383-1386.
39. Bahrami, A., & Hejazi, P. (2013). Electrostatic immobilization of pectinase on negatively charged AOT-Fe3O4 nanoparticles. *J. Mol. Catal. B: Enzym.*, *93*, 1-7.
40. Roth, H. C., Schwaminger, S. P., Peng, F., & Berensmeier, S. (2016). Immobilization of cellulase on magnetic nanocarriers. *ChemistryOpen*, *5*(3), 183-187.

41. Schwaminger, S. P., Fraga-García, P., Selbach, F., Hein, F. G., Fuß, E. C., Surya, R., … Berensmeier, S. (2017). Bio-nano interactions: cellulase on iron oxide nanoparticle surfaces. *Adsorption*, *23*(2), 281-292.
42. Zhu, H., Pan, J., Hu, B., Yu, H.-L., & Xu, J.-H. (2009). Immobilization of glycolate oxidase from Medicago falcata on magnetic nanoparticles for application in biosynthesis of glyoxylic acid. *J. Mol. Catal. B: Enzym.*ÿ *61*(3), 174-179.
43. Johnson, A. K., Zawadzka, A. M., Deobald, L. A., Crawford, R. L., & Paszczynski, A. J. (2008). Novel method for immobilization of enzymes to magnetic nanoparticles. *J. Nanoparticle Res.*, *10*(6), 1009-1025.
44. Rahdar, S., Rahdar, A., Ahmadi, S., & Trant, J. F. (2019). Adsorption of bovine serum albumin (BSA) by bare magnetite nanoparticles with surface oxidative impurities that prevent aggregation. *Can. J. Chem.*, *97*(8), 577-583.
45. Tentori, F., Bavaro, T., Brenna, E., Colombo, D., Monti, D., Semproli, R., & Ubiali, D. (2020). Immobilization of old yellow enzymes via covalent or coordination bonds. *Catalysts*, 260, *10*(2).
46. Dyal, A., Loos, K., Noto, M., Chang, S. W., Spagnoli, C., Shafi, K. V., … Gross, R. A. (2003). Activity of Candida rugosa lipase immobilized on gamma-Fe2O3 magnetic nanoparticles. *J. Am. Chem. Soc.*, *125*(7), 1684-1685.
47. Shaw, S. - Y., Chen, Y. - J., Ou, J. - J., & Ho, L. (2006). Preparation and characterization of Pseudomonas putida esterase immobilized on magnetic nanoparticles. *Enzyme Microb. Technol.*, 2006.*39*(5), 1089-1095.
48. Muley, A. B., Mulchandani, K. H., & Singhal, R. S. (2020). Chapter Three - Immobilization of enzymes on iron oxide magnetic nanoparticles: Synthesis, characterization, kinetics and thermodynamics. In C.V. Kumar (Ed.), *Methods Enzymol.* (pp. 39-79). Academic Press.
49. Li, H., Xiao, W., Xie, P., & Zheng, L. (2018). Co-immobilization of enoate reductase with a cofactor-recycling partner enzyme. *Enzyme Microb. Technol.*, *109*, 66-73.
50. Jordan, J., Kumar, C. S. S. R., & Theegala, C. (2011). Preparation and characterization of cellulase-bound magnetite nanoparticles. *J. Mol. Catal. B: Enzym.*, *68*(2), 139-146.
51. Jordan, J., & Theegala, C. (2014). Probing the limitations for recycling cellulase enzymes immobilized on iron oxide (Fe3O4) nanoparticles. *Biomass Conversion Biorefinery*, *4*(1), 25-33.

SUPPORTING INFORMATION

Additional supporting information may be found online in the Supporting Information section at the end of the article.

How to cite this article: Zanker, A. A., Ahmad, N., Son, T. H., Schwaminger, S. P., & Berensmeier, S. (2021). Selective ene-reductase immobilization to magnetic nanoparticles through a novel affinity tag. *Biotechnol J*, 16, e2000366. https://doi.org/10.1002/biot.202000366